Title
Proximity of excitatory and inhibitory axon terminals adjacent to pyramidal cell bodies provides a putative basis for nonsynaptic interactions

Journal
Proceedings of the National Academy of Sciences of the United States of America, 106(24)

ISSN
0027-8424

Authors
Merchán-Pérez, Angel
Rodriguez, José-Rodrigo
Ribak, Charles E
et al.

Publication Date
2009-06-16

DOI
10.1073/pnas.0900330106

Proximity of excitatory and inhibitory axon terminals adjacent to pyramidal cell bodies provides a putative basis for nonsynaptic interactions

Angel Merchán-Pérez[a,1], José-Rodrigo Rodriguez[b], Charles E. Ribak[c], and Javier DeFelipe[b,1]

[a]Department of Anatomy I, School of Medicine, Universidad Complutense, 28040 Madrid, Spain; [b]Instituto Cajal, Consejo Superior de Investigaciones Científicas, Avenida Doctor Arce 37, 28002 Madrid, Spain; and [c]Department of Anatomy and Neurobiology, School of Medicine, University of California at Irvine, Irvine, CA 92697-1275

Edited by Edward G. Jones, University of California, Davis, CA, and approved April 28, 2009 (received for review January 12, 2009)

Although pyramidal cells are the main excitatory neurons in the cerebral cortex, it has recently been reported that they can evoke inhibitory postsynaptic currents in neighboring pyramidal neurons. These inhibitory effects were proposed to be mediated by putative axo-axonic excitatory synapses between the axon terminals of pyramidal cells and perisomatic inhibitory axon terminals [Ren M, Yoshimura Y, Takada N, Horibe S, Komatsu Y (2007) *Science* 316:758–761]. However, the existence of this type of axo-axonic synapse was not found using serial section electron microscopy. Instead, we observed that inhibitory axon terminals synapsing on pyramidal cell bodies were frequently apposed by terminals that established excitatory synapses with neighbouring dendrites. We propose that a spillover of glutamate from these excitatory synapses can activate the adjacent inhibitory axo-somatic terminals.

axo-axonic synapses | glutamate spillover | interpyramidal inhibition | perisomatic innervation | serial electron microscopy

Pyramidal cells are the most abundant cortical neurons and although they are projection neurons, their axons give rise to axonal collaterals before leaving the cortex, producing a rich local intracortical plexus (1). In general, the pyramidal cell's soma and axon initial segment receive only symmetric (inhibitory) synapses from axon terminals of GABAergic interneurons, whereas its dendrites receive synaptic inputs from axon terminals forming both symmetric and asymmetric (excitatory) synapses. The latter type of synapse is mainly located on dendritic spines and such synapses arise from multiple intrinsic and extrinsic sources (2). Many studies have shown that pyramidal neurons are glutamatergic and that they exert a fundamental excitatory function in cortical circuits (3). Indeed, these neurons represent the primary source of cortical excitatory synapses, and in turn, dendritic spines of pyramidal cells are the target of most excitatory synapses (2).

This traditional view has recently been challenged by the discovery that pyramidal neurons in layer II/III of the mouse visual cortex exert an inhibitory influence on neighboring pyramidal cells through the direct activation of inhibitory GABAergic axon terminals forming axo-somatic synapses (4) (referred to here as "axo-somatic terminals"). Thus, single-action potentials generated in a pyramidal neuron can produce inhibitory postsynaptic currents (IPSCs) in nearby pyramidal cells with short latencies, which are in many cases comparable to monosynaptic connections. These responses are abolished by both non-NMDA and $GABA_A$ receptor antagonists, suggesting that they are disynaptic. Other electrophysiological and pharmacological evidence makes it unlikely that these IPSCs are mediated by the conventional activation of inhibitory interneurons, generating somatic action potentials that subsequently spread through the axonal tree. Instead, they seem to take place in the immediate vicinity of the pyramidal cell body.

Because these data imply a very close relationship between excitatory and perisomatic inhibitory terminals, the spatial arrangement of these 2 kinds of boutons has been studied using immunocytochemistry and confocal microscopy (4). Data by Ren et al. (4) revealed that these 2 types of terminals were very frequently in close apposition. Accordingly, it was concluded that these interpyramidal IPSCs were probably mediated by pyramidal axon terminals that formed axo-axonic synapses with inhibitory terminals, which in turn made axo-somatic synapses on the soma of neighboring pyramidal cells. In this disynaptic pathway, the first synapse (axo-axonic) would be glutamatergic and mediated by kainate and AMPA receptors, whereas the second synapse (axo-somatic) would be GABAergic and mediated by $GABA_A$ receptors.

The main drawback of this interpretation is that such axo-axonic synapses between glutamatergic terminals and GABAergic terminals have never been described in the cerebral cortex (5–11). Therefore, the structural basis for these particular interpyramidal connections remains uncertain (12, 13). However, ultrastructural studies have generally been carried out on single sections or partial reconstructions, and they have focused mainly on the axon terminals forming axo-somatic synapses onto pyramidal cells. Moreover, more recent studies examining axo-somatic terminals have used techniques that require the labeling of the axon terminals with 3,3′ diaminobenzidine tetrahydrochloride (DAB) (14). Unfortunately, these techniques produce intense intracellular labeling that may mask synaptic specializations. Thus, for these reasons it is possible that the existence of these putative axo-axonic synapses has passed unnoticed.

The unequivocal identification of synaptic membrane specializations requires conventional electron microscopy, and ideally, 3-dimensional reconstructions. Hence, we have undertaken an ultrastructural study using serial sections to fully reconstruct axo-somatic terminals in search of the morphological substrate of these interpyramidal inhibitory effects. As a complementary approach, we have also used immunofluorescence and pre-embedding immunoelectron microscopy to examine markers of GABAergic and glutamatergic terminals. We used an antibody against the vesicular glutamate transporter 1 (VGluT1) as a marker of glutamatergic terminals (14, 15), and either an anti-GABA transporter 1 (GAT1) or an anti-vesicular GABA transporter (VGAT) antibody as markers of GABAergic terminals (16–18). Finally, as such synapse-like contacts might be found in particular cortical regions or species, or during certain developmental stages, we have analyzed the same cortical re-

Author contributions: C.E.R. and J.D. designed research; A.M.-P. and J.-R.R. performed research; A.M.-P. and J.-R.R. analyzed data; and A.M.-P., C.E.R., and J.D. wrote the paper.

The authors declare no conflict of interest.

This article is a PNAS Direct Submission.

[1]To whom correspondence may be addressed. E-mail: defelipe@cajal.csic.es or amerchan@med.ucm.es.

This article contains supporting information online at www.pnas.org/cgi/content/full/0900330106/DCSupplemental.

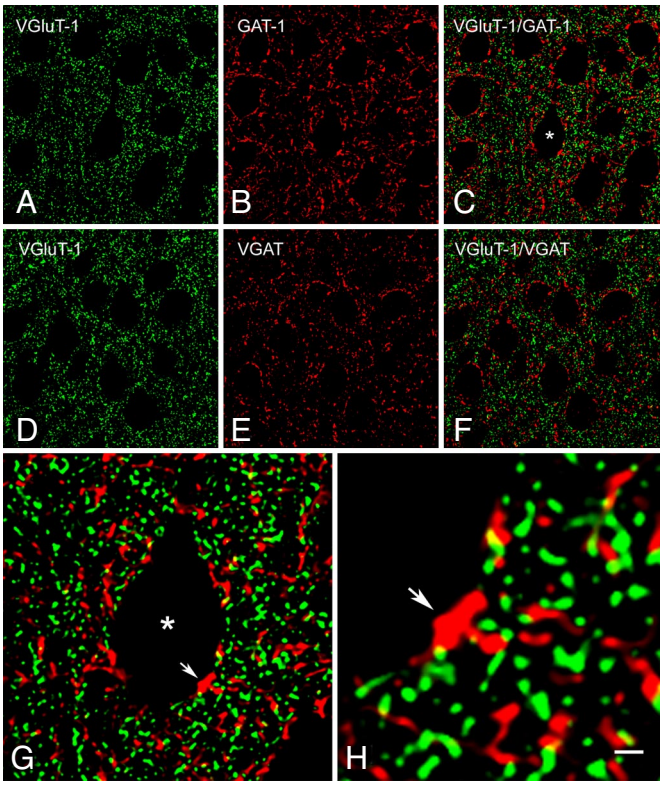

Fig. 1. Single-plane confocal images showing immunostaining for VGluT1, GAT1, and VGAT in layer II of the mouse visual cortex. (*A* and *D*) VGluT1-ir appears in punctate structures distributed in the neuropil, as well as around unlabeled pyramidal cell somata and apical dendrites. (*B* and *E*) GAT1- and VGAT-ir are also present in puncta around cell bodies and in the neuropil. Merging of the paired images (*A* and *B*) and (*D* and *E*) shows that VGluT1 and GAT1 (*C*), or VGluT1 and VGAT (*F*), do not colocalize, even though numerous VGluT1-positive puncta are contiguous to GAT1- or VGAT-positive puncta. (*G*) Higher magnification of the pyramidal cell soma labeled with an asterisk in (*C*). The close apposition between some of the punctate structures that surround the cell body is clearly evident. The yellow, partially overlapping areas of contiguous red (GAT1) and green (VGluT1) profiles, suggest the intimate apposition of the 2 types of terminals. The arrow in (*G*) and (*H*) points to the same GAT1-positive terminal that is apposed to the cell soma and to several VGluT1-positive puncta. [Scale bar: 10 μm from (*A*) to (*F*), 3 μm in (*G*), and 1 μm in (*H*).]

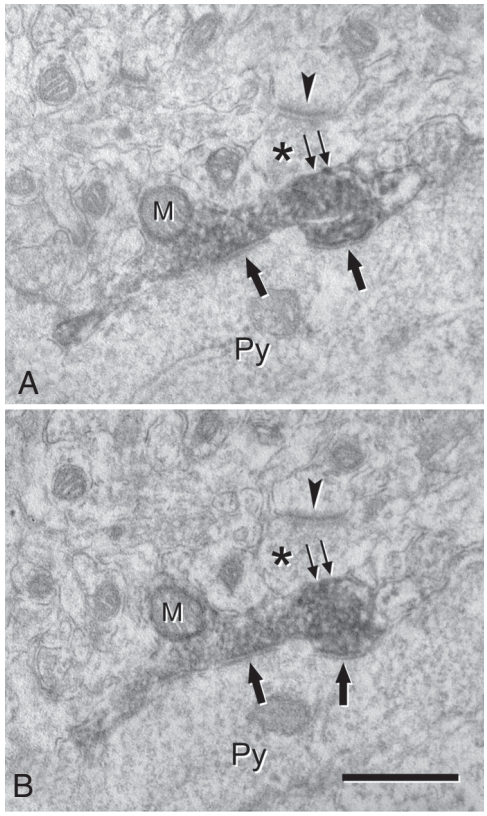

Fig. 2. (*A* and *B*) Ultrastructural localization of VGAT in an axon terminal that makes a symmetric synapse with a pyramidal cell soma (Py). (*A*) and (*B*) are 2 consecutive ultrathin sections. The labeled terminal is filled with the dark DAB precipitate that obscures the internal details, although a mitochondrion (M), synaptic vesicles and 2 axo-somatic synapses (*single arrows*) can be distinguished. An unlabeled terminal (*asterisks*) is apposed to the labeled terminal and it makes an asymmetric (excitatory) synapse with a nearby dendritic element, probably a dendritic spine. The arrowheads point to the postsynaptic density of the asymmetric synapse. Note that at the membrane of the VGAT-ir terminal adjacent to the unlabeled terminal (*double arrows*) it is hard to ascertain whether a putative synaptic contact is present because the DAB reaction product is too electron dense. (Scale bar, 0.5 μm.)

gion, mouse strain, and age as those originally examined by Ren et al. (4).

Results

VGluT1 immunoreactivity (ir) was exclusively associated with punctate structures widely distributed in the neuropil and in close apposition to unlabeled cell bodies of different shapes and sizes. Virtually all pyramidal cell somata and proximal processes in layers II to VI were outlined by VGluT1-positive puncta (Fig. 1 *A* and *D*). This pattern of immunostaining was very similar to that displayed for the GABAergic markers GAT1 and VGAT, with numerous puncta evident in the neuropil and around the cell bodies (Fig. 1 *B* and *E*). Despite this similar distribution, double-labeling experiments showed that VGluT1-ir did not colocalize with either of the 2 GABAergic markers (Fig. 1 *C*, *F–H*) [See also supporting information (SI) Movie S1]. Nevertheless, VGluT1-positive puncta were often contiguous to VGAT- or GAT1-positive puncta, both in the neuropil and around the neuronal somata (see Fig. 1 *G* and *H* and Movie S1).

At the electron microscopic level, a total of 119 VGluT1-, 108 VGAT-, and 145 GAT1-positive puncta were examined. VGluT1-positive puncta were found to be axon terminals establishing asymmetric synapses with dendritic shafts and dendritic spines in the neuropil. However, they were never seen to make synaptic junctions with cell somata nor were axo-axonic synapses established with any other terminals. VGAT- and GAT1-positive puncta were also found to be axon terminals, consistent with previous reports (14, 16–18). These terminals established symmetric synapses with pyramidal cell somata (Fig. 2) and with dendrites in the neuropil. Indeed, VGAT- and GAT1-positive axon terminals never established axo-axonic synapses with other labeled or unlabelled axon terminals. The presynaptic densities of axon terminals labeled for VGluT1, GAT1, or VGAT were often difficult to visualize because of the DAB precipitate that masked the synaptic specializations. Consequently, 2 or more consecutive sections were usually needed to unequivocally identify synapses (see Fig. 2 *A* and *B*), although in up to a quarter of the labeled terminals it was not possible to verify whether synaptic specializations were present (see *double arrows* in Fig. 2 *A* and *B*). In addition, the use of an extended series of sections in this material was difficult to interpret because immunoreactivity was restricted to the surface of sections due to the limited penetration of the antibodies. Moreover, the preservation of the tissue was not optimal at the surface. Therefore, to confirm whether axo-axonic synapses were present in the perisomatic region of pyramidal cells, it was necessary to analyze material

NEUROSCIENCE

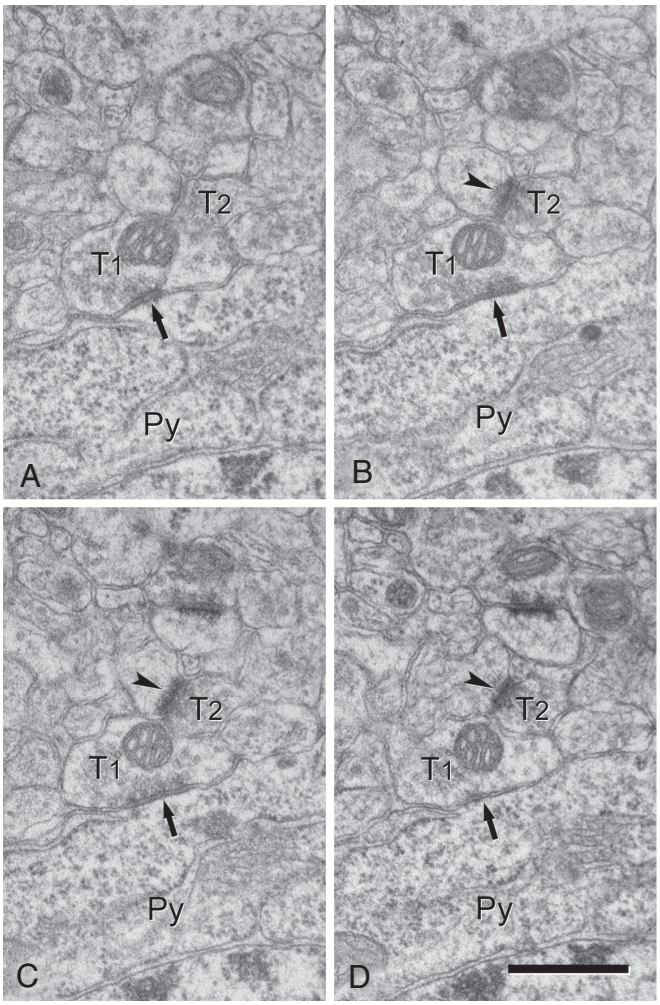

Fig. 3. (*A–D*) Serial ultrathin sections showing an axo-somatic symmetric (inhibitory) synapse (*arrows*) and an adjacent axo-dendritic asymmetric (excitatory) synapse (*arrowheads*). Axon terminals forming symmetric and asymmetric synapses are indicated as T1 and T2, respectively. T2 is directly apposed to the axo-somatic bouton T1. Note that the postsynaptic density of the asymmetric synapse (*arrowheads*) is close to the membrane of the axo-somatic terminal (T1) and that there are no glial or neural profiles interposed. Py, pyramidal cell soma. (Scale bar, 0.5 μm.)

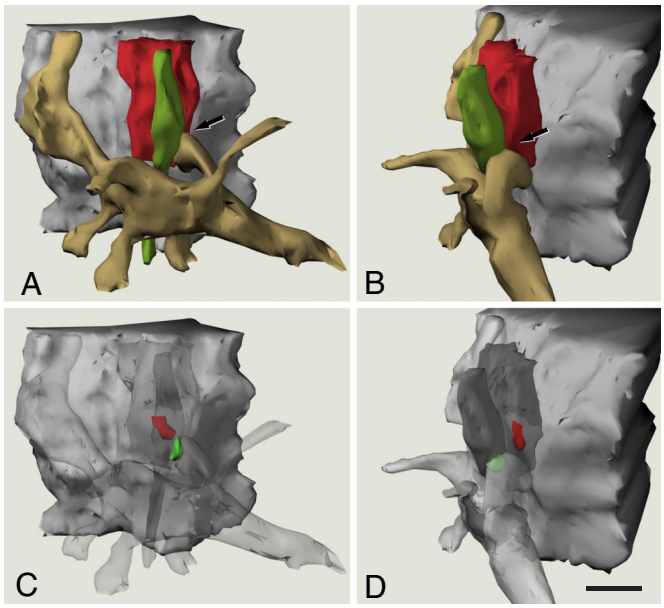

Fig. 4. Three-dimensional reconstruction of an axo-somatic terminal and a neighbouring axo-dendritic synapse. (*A*) and (*B*) are 2 views at different angles (a 55° clockwise rotation through the vertical axis) to show a portion of a pyramidal cell body (*gray*), an axo-somatic inhibitory terminal (*red*), an excitatory axon terminal (*green*), and a spiny dendritic segment (*pale brown*). Note the close apposition between the axo-somatic terminal, the excitatory axon terminal, and a dendritic spine in the region indicated by arrows. (*C*) and (*D*) are paired with (*A*) and (*B*), respectively, where the axon terminals and dendritic structures have been made transparent to show the location of the postsynaptic densities (PSDs) associated with the 2 axon terminals. The PSD of the inhibitory synapse (*red*) is located in the pyramidal cell body, in front of the axo-somatic terminal. The PSD of the excitatory synapse (*green*) is located in the dendritic spine apposed to the excitatory axon terminal. This excitatory synapse is in close proximity to the inhibitory axo-somatic terminal. Notice that no axo-axonic synapse was observed between the 2 axon terminals. (Scale bar, 0.5 μm.)

that had not been immunostained to avoid any possible masking of synaptic specializations by the chromogen. Hence, we completely reconstructed axon terminals that formed synapses with the somata of pyramidal cells in serial sections from unstained tissue that was specifically prepared for conventional electron microscopy.

In this material, we succeeded in completely reconstructing 48 axo-somatic terminals that formed symmetric synapses on the soma of pyramidal cells. While none of them established axo-axonic synapses, 19 of the 48 axo-somatic terminals (39.6%) had another axon terminal directly apposed to them (without any intervening neural or glial processes). Among these 19 axo-somatic terminals, 15 had a single terminal apposed to them, while 2 had two terminals, and the remaining 2 had three terminals. All of these apposed terminals established asymmetric synapses with adjacent dendrites or dendritic spines (Figs. 3 and 4, Figs. S1 and S2).

The localization of the axo-dendritic synapses with respect to the membrane of the axo-somatic terminals was variable, but in many cases they were so close that the asymmetric axo-dendritic synapse and the axo-somatic terminal were almost in contact (see Figs. 3 and 4 and Fig. S1). We measured the minimum distance through the extracellular space between the edge of the PSD of the axo-dendritic asymmetric synapses and the membrane of the adjacent axo-somatic terminal, which ranged from 0.0126 to 0.1945 μm (mean $\pm$ SD, 0.0689 $\pm$ 0.0609 μm). We also measured the minimum distance through the extracellular space between the edges of PSDs of the asymmetric axo-dendritic synapses and the adjacent symmetric axo-somatic synapse, which ranged from 0.1747 to 2.5061 μm (mean $\pm$ SD, 0.7667 $\pm$ 0.4692 μm). All measurements were obtained from single sections and were not estimated from 3-dimensional reconstructions. The distribution of both these measurements is shown in Fig. 5.

Discussion

The results of our confocal microscopy analysis are compatible with earlier findings (4) because virtually all of the cell bodies of pyramidal neurons in layer II of the visual cortex were surrounded by glutamatergic (VGluT1-positive) and GABAergic (GAT1- or VGAT-positive) terminals at the light microscopic level. Indeed, both types of puncta were frequently apposed to one another. Data by Ren et al. (4) indicated that more than 50% of terminals expressing the GABA synthesizing enzymes glutamic acid decarboxylase 65 and 67 (GAD65/67) were apposed by boutons expressing VGluT1. Based on this spatial relationship of perisomatic boutons, and in conjunction with electrophysiological and

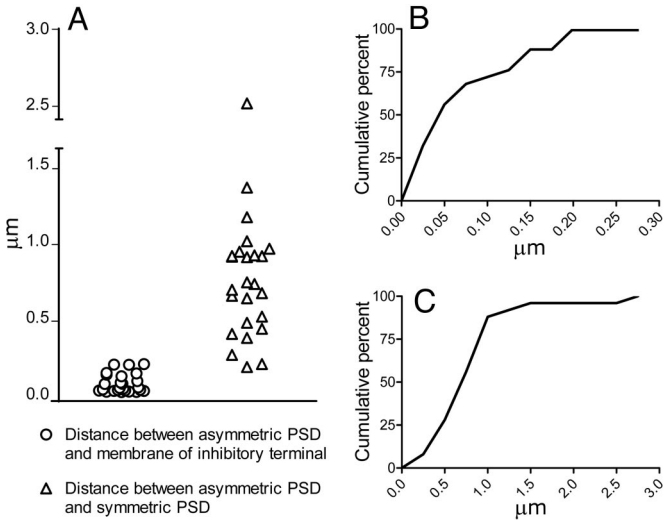

Fig. 5. Distribution of measurements derived from the 19 of the 48 axo-somatic terminals that were apposed by an excitatory terminal. (*A*) Comparative distribution of the shortest distances between the PSDs of asymmetric synapses and the membrane of the adjacent axo-somatic terminal (*circles*), and of the distances between the PSDs of asymmetric synapses and of the symmetric axo-somatic synapses (*triangles*). (*B*) Cumulative distribution of the minimum distances between the PSDs of axo-dendritic synapses and the membrane of the neighbouring axo-somatic terminals. All distances are smaller than 0.2 μm and while 72% are smaller than 0.1 μm, 56% are less than 0.05 μm. (*C*) Cumulative distribution of the minimum distances between the PSDs of adjacent axo-dendritic asymmetric and axo-somatic symmetric synapses. Note that the distances in (*C*) are 10 times that in (*B*).

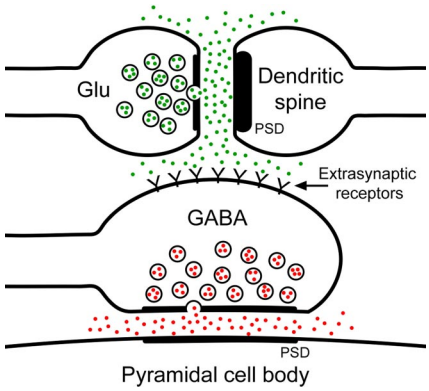

Fig. 6. Schematic representation of the relationship between excitatory and inhibitory synapses in the perisomatic region of a pyramidal cell. A glutamatergic terminal (Glu) establishes an excitatory synapse with a dendritic spine, which is recognized at the electron microscope level by the presence of a thick PSD (asymmetric synapse). These terminal and spine are apposed to the membrane of an axo-somatic GABAergic terminal (GABA) that establishes an inhibitory synapse with the cell body of the pyramidal cell (thinner PSD; symmetric synapse). The spillover of glutamate (*green dots*) from the excitatory synapse might activate the extrasynaptic receptors located on the membrane of the axo-somatic terminal. Finally, the activation of these receptors might cause the release of GABA (*red dots*) from the axo-somatic terminal.

pharmacological data, the existence of axo-axonic excitatory synapses with GABAergic terminals was proposed. The electron microscopic data in the present study confirm the frequent apposition of excitatory and inhibitory perisomatic terminals, but not the existence of axo-axonic synapses between them. Given that the probability of detecting IPSCs between pyramidal neuron pairs is rather high (28%) (4), these putative axo-axonic synapses should be a common structural arrangement. However, we did not find any examples of this type of synapse in our serial section analysis of 48 examined axo-somatic terminals. Similarly, in a previous study of the rat somatosensory cortex, VGluT1-ir was found around the profiles of the soma and proximal dendritic segments of virtually all pyramidal neurons (14). Furthermore, these terminals were closely apposed to parvalbumin-ir inhibitory terminals. Our electron microscopy studies showed that VGluT1-positive terminals apposed to the pyramidal cell bodies never established axo-somatic or axo-axonic synapses, but rather they formed axo-dendritic synapses with nearby dendritic shafts and spines (14).

An alternative explanation to account for the inhibition between pyramidal neurons is that there is spillover of glutamate from the asymmetric synapses onto the membranes of the apposed GABAergic axo-somatic terminals. For interpyramidal inhibition to occur, enough glutamate must diffuse from the synaptic cleft to reach the membrane of the apposed GABAergic terminal to evoke a response. In turn, this response would lead to the release of GABA and the initiation of an IPSC at the pyramidal neuron (Fig. 6). The distance between the source and target, and the geometry of the extracellular space, are among the most important physical constraints affecting the possibility of neurotransmitter diffusion (19, 20). The presence of glial processes between the neighboring terminals would also affect the diffusion of neurotransmitters, because such processes would act as a physical barrier and play a major role in the uptake of transmitter molecules (21, 22). In our sample, 39.6% of the axo-somatic terminals were directly apposed by an excitatory axon terminal making an asymmetric synapse onto a neighboring dendrite. Moreover, in all these cases the distance between the asymmetric (excitatory) synapse and the membrane of the axo-somatic (inhibitory) terminal, although variable, was always less than 0.2 μm. The absence of interposed glial processes (with the capacity for neurotransmitter uptake) between these terminals would facilitate glutamate reaching the membrane of the axo-somatic terminal.

Several models have addressed the issue of the spillover of glutamate from the synaptic cleft in the hippocampus. Some of these models seem to indicate that the concentration of glutamate at 0.1 μm from the release point would reach a peak between 1 mM and 10 mM. At 0.2 μm of distance, the glutamate peak would be still about 0.8 mM, while it would fall below 0.1 mM at 0.5 μm of distance (23, 24). All these transients would take place within the first millisecond from release, and thus they would take place at a spatial and temporal scale that support our hypothesis (see also ref. 25).

The glutamate released into the extracellular space should interact with non-NMDA receptors present along the membrane of the GABAergic terminal, leading to its activation. These kinds of receptors have been identified in the visual cortex by electrophysiological and pharmacological methods (4). Furthermore, ≈40% of GAD65/67-positive terminals also expressed the glutamate receptor subunit GluR5, a component of non-NMDA receptors, in mechanically dissociated preparations (4). Indeed, the activation of GABAergic terminals by glutamate could be a widespread mechanism, as a similar facilitatory effect on the release of GABA mediated by kainate receptors has also been described in the prefontal cortex (26, 27). We must also consider the possibility that the diffusing glutamate (and other compounds) may reach the inhibitory PSD, and not just the cell membrane of the terminal, evoking the release of GABA. However, this seems unlikely given the relatively larger distances between the excitatory and inhibitory PSDs. Thus, the possible influence of this glutamate on

excitatory and inhibitory terminals seems to be minimal at the level of their PSDs.

Our data, taken together with the electrophysiological data of Ren et al. (4), suggest a previously unrecorded interpretation of the function for inhibitory axo-somatic synapses. The tight spatial association of an excitatory axo-dendritic synapse with an axo-somatic inhibitory terminal would mimic the behavior of a hypothetical axo-axonic synapse, provided the 2 elements were close enough for the diffusion of glutamate (see above). Thus, the spillover of neurotransmitter may represent a new and widespread mechanism by which cortical pyramidal neurons can interact with interneurons. Indeed, this interaction would represent an intermediate situation between conventional synapses and volume transmission (28), because the spatial disposition of these perisomatic excitatory and inhibitory terminals may allow transmission with a time course comparable to that of traditional chemical synapses. Furthermore, the extrasynaptic activation of the inhibitory axo-somatic terminals would depend on the activation of the neighboring excitatory synapse, rather than representing a diffuse and nonspecific phenomenon.

Materials and Methods

Serial Section Electron Microscopy. Five male C57 mice 26 days of age were administered a lethal i.p. injection of sodium pentobarbital (40 mg/kg) and then were intracardially perfused with saline solution followed by 1% paraformaldehyde and 1.25% glutaraldehyde in 0.12M phosphate buffer, pH 7.4 (PB) (29). The heads were left overnight in the same fixative at 4 °C, and the brains were removed the next morning and postfixed in fresh fixative for 1 additional day. Thereafter, the brains were washed in several changes of 0.12 M PB and vibratome sections (150-μm thick) were selected from the primary visual cortex with the help of the Paxinos and Franklin atlas (30). Consecutive sections were either stained with the Nissl method or osmicated and flat-embedded in Araldite to perform electron microscopy (31).

Serial ultrathin sections (70-nm thick) were taken from layer II of the visual cortex, which was previously identified and located in 1-μm thick semithin plastic sections stained with toluidine blue. The ultrathin sections were collected on single-slot Formvar-coated grids and routinely stained with uranyl acetate and lead citrate. To completely reconstruct axo-somatic synapses on the cell bodies of pyramidal cells, we used strings of serial sections, which ranged from 9 to 32 consecutive sections (mean 29). Axosomatic boutons that made symmetric synapses (9) on randomly chosen pyramidal neurons (identified by the presence of an apical dendrite) were photographed digitally on the electron microscope (Jeol 1200 EX II electron microscope, Jeol USA Inc.). Microphotographs were mounted, calibrated and serially aligned with the Reconstruct software (32). This software was also used for the semiautomatic, 3-dimensional reconstruction of axo-somatic boutons. In this way, a total of 48 axo-somatic boutons were fully reconstructed.

Brain tissue shrinks during processing for electron microscopy, especially during osmication and plastic embedding. Thus, to estimate the shrinkage in our samples we measured the surface area and thickness of the vibratome sections with Stereo Investigator (MBF Bioscience) both before and after they were processed for electron microscopy (33). The surface area after processing was divided by the value before processing to obtain an area shrinkage factor (p^2) of 0.8956. The linear shrinkage factor for measurements in the plane of the section, p, was therefore 0.9464. The shrinkage factor in the z-axis was 0.9512. All measured distances were corrected to obtain an estimate of the preprocessing values.

Immunofluorescence and Pre-Embedding Immunoelectron Microscopy. As a complementary approach, we have also used immunofluorescence and pre-embedding immunoelectron microscopy to examine markers of GABAergic and glutamatergic terminals. Five additional C57 male mice of the same age were used for these experiments and they were processed in the same way as above except that the fixative used was 4% paraformaldehyde in PB. Free-floating vibratome sections (100-μm thick) were processed for immunofluorescence or immunoelectron microscopy, while adjacent sections were also collected and Nissl stained.

For double-immunofluorescence labeling we used a guinea-pig antibody against the vesicular glutamate transporter 1 (VGluT1, diluted 1/2500) as a marker of glutamatergic terminals (15), and either a rabbit anti-GAT1 or a rabbit anti-VGAT antibody (diluted 1/500 and 1/2,000, respectively), as markers of GABAergic terminals (16, 18). The VGluT1 and GAT1 antibodies were obtained from Millipore Corp., whereas the VGAT antibody was supplied by Synaptic Systems GmbH. The primary antibodies were diluted in PB containing 0.25% Triton X-100 and 3% normal goat serum and the sections were incubated for 36 h at 4 °C. Secondary antibodies conjugated with Alexa fluorochromes (Invitrogen) were used at a dilution of 1/200, and they were incubated for 1 h at room temperature. The anti guinea-pig secondary antibody was Alexa 488-conjugated (green emission color), while the anti rabbit secondary antibody was conjugated with Alexa 594 (red emission color). Finally, the sections were photographed on a Leica DMI 600B laser scanning confocal microscope, and the visualization and deconvolution of the images was performed with Imaris (Bitplane AG) and Autodeblur (Media Cybernetics Inc.) softwares.

For pre-embedding immunoelectron microscopy we used the same primary antibodies at the same dilutions and incubation times as above, but in the absence of Triton X-100. The corresponding biotinylated secondary antibodies (diluted 1/200), were visualized using an avidin-biotin-peroxidase complex (Vector Laboratories Inc.) and DAB. The sections were then osmicated, embedded in Araldite and processed for electron microscopy as above.

All animals were handled in accordance with the guidelines for animal research set out in the European Community Directive 86/609/EEC. All procedures were also approved by the local ethics committee of the Spanish National Research Council.

ACKNOWLEDGMENTS. We thank A.I. García and I. Fernaud for technical assistance. This work was supported by grants from Centro de Investigación Biomédica en Red sobre Enfermedades Neurodegenerativas, the EU 6th Framework Program (PROMEMORIA LSHM-CT-2005–512012), the Spanish Ministry of Science and Technology (grant BFU2006–13395) and the Cajal Blue Brain Project.

1. DeFelipe J, Jones EG (1988) *Cajal on the Cerebral Cortex* (Oxford Univ Press, New York).
2. DeFelipe J, Fariñas I (1992) The pyramidal neuron of the cerebral cortex: Morphological and chemical characteristics of the synaptic inputs. *Prog Neurobiol* 39: 563–607.
3. Spruston N (2008) Pyramidal neurons: Dendritic structure and synaptic integration. *Nat Rev Neurosci* 9:206–221.
4. Ren M, Yoshimura Y, Takada N, Horibe S, Komatsu Y (2007) Specialized inhibitory synaptic actions between nearby neocortical pyramidal neurons. *Science* 316:758–761.
5. Ribak CE (1978) Aspinous and sparsely-spinous stellate neurons in the visual cortex of rats contain glutamic acid decarboxylase. *J Neurocytol* 7:461–478.
6. Freund TF, Martin KA, Smith AD, Somogyi P (1983) Glutamate decarboxylase-immunoreactive terminals of Golgi-impregnated axoaxonic cells and of presumed basket cells in synaptic contact with pyramidal neurons of the cat's visual cortex. *J Comp Neurol* 221:263–278.
7. Hendry SH, Houser CR, Jones EG, Vaughn JE (1983) Synaptic organization of immunocytochemically identified GABA neurons in the monkey sensory-motor cortex. *J Neurocytol* 12:639–660.
8. Peters A, Sethares C, Harriman KM (1990) Different kinds of axon terminals forming symmetric synapses with the cell bodies and initial axon segments of layer II/III pyramidal cells. II. Synaptic junctions. *J Neurocytol* 19:584–600.
9. Peters A, Palay SL, Webster H (1991) *The Fine Structure of the Nervous System. Neurons and their Supporting Cells* (Oxford Univ Press, New York).
10. Fariñas I, DeFelipe J (1991) Patterns of synaptic input on corticocortical and corticothalamic cells in the cat visual cortex. I. The cell body. *J Comp Neurol* 304:53–69.
11. Lund JS, Griffiths S, Rumberger A, Levitt JB (2001) Inhibitory synapse cover on the somata of excitatory neurons in macaque monkey visual cortex. *Cereb Cortex* 11:783–795.
12. Connors BW, Cruikshank SJ (2007) Bypassing interneurons: inhibition in neocortex. *Nat Neurosci* 10:808–810.
13. Pinheiro PS, Mulle C (2008) Presynaptic glutamate receptors: physiological functions and mechanism of action. *Nat Rev Neurosci* 9:423–436.
14. Alonso-Nanclares L, et al. (2004) Perisomatic glutamatergic axon terminals: A novel feature of cortical synaptology revealed by vesicular glutamate transporter 1 immunostaining. *Neuroscience* 123:547–556.
15. Fremeau RT, Voglmaier S, Seal RP, Edwards RH (2004) VGLUTs define subsets of excitatory neurons and suggest novel roles for glutamate. *Trends Neurosci* 27:98–103.
16. Minelli A, Brecha NC, Karschin C, DeBiasi S, Conti F (1995) GAT1, a high-affinity GABA plasma membrane transporter, is localized to neurons and astroglia in the cerebral cortex. *J Neurosci* 15:7734–7746.
17. Yan XX, Cariaga WA, Ribak CE (1997) Immunoreactivity for GABA plasma membrane transporter, GAT-1, in the developing rat cerebral cortex: transient presence in the somata of neocortical and hippocampal neurons. *Dev Brain Res* 99:1–19.

18. Minelli A, Alonso-Nanclares L, Edwards RH, DeFelipe J, Conti F (2003) Postnatal development of the vesicular GABA transporter in rat cerebral cortex. *Neuroscience* 117:337–346.
19. Rusakov DA, Kullmann DM (1998) Geometric and viscous components of the tortuosity of the extracellular space in the brain. *Proc Natl Acad Sci USA* 95:8975–8980.
20. Nicholson C (2005) Factors governing diffusing molecular signals in brain extracellular space. *J Neural Transm* 112:29–44.
21. Oliet SHR, Piet R, Poulain DA (2001) Control of glutamate clearance and synaptic efficacy by glial coverage of neurons. *Science* 292:923–926.
22. Piet R, Vargová L, Syková E, Poulain DA, Oliet SHR (2004) Physiological contribution of the astrocytic environment of neurons to intersynaptic crosstalk. *Proc Natl Acad Sci USA* 101:2151–2155.
23. Rusakov DA, Kullmann DM (1998) Extrasynaptic glutamate diffusion in the hippocampus: Ultrastructural constraints, uptake, and receptor activation. *J Neurosci* 18:3158–3170.
24. Rusakov DA, Kullmann DM, Stewart MG (1999) Hippocampal synapses: Do they talk to their neighbours? *Trends Neurosci* 22:382–388.
25. Zheng K, Scimemi A, Rusakov DA (2008) Receptor actions of synaptically released glutamate: the role of transporters on the scale from nanometers to microns. *Biophys J* 95:4584–4596.
26. Mathew SS, Pozzo-Miller L, Hablitz JJ (2008) Kainate modulates presynaptic GABA release from two vesicle pools. *J Neurosci* 28:725–731.
27. Mathew SS, Hablitz JJ (2008) Calcium release via activation of presynaptic IP3 receptors contributes to kainate-induced IPSC facilitation in rat neocortex. *Neuropharmacology* 55:106–116.
28. Fuxe K, et al. (2007) From the Golgi-Cajal mapping to the transmitter-based characterization of the neuronal networks leading to two modes of brain communication: Wiring and volume transmission. *Brain Res Rev* 55:17–54.
29. Palay SL, Sotelo C, Peters A, Orkand PM (1968) The axon hillock and the initial segment. *J Cell Biol* 38:193–201.
30. Paxinos G, Franklin KBJ (2001) *The Mouse Brain in Stereotaxic Coordinates*, Second edition (Academic, San Diego, CA).
31. DeFelipe J, Fairén A (1993) A simple and reliable method for correlative light and electron microscopic studies. *J Histochem Cytochem* 41:769–772.
32. Fiala JC (2005) Reconstruct: A free editor for serial section microscopy. *J Microsc* 218:52–61.
33. Oorschot DE, Peterson DA, Jones DG (1991) Neurite growth from, and neuronal survival within, cultured explants of the nervous system: a critical review of morphometric and stereological methods, and suggestions for the future. *Prog Neurobiol* 37:525–546.